C-Terminal Cleavage of ΔNp63α Is Associated with TSA-Induced Apoptosis in Immortalized Corneal Epithelial Cells

Danielle M. Robertson, Su-Inn Ho, and H. Dwight Cavanagh

Purpose. In the central human corneal epithelium, loss of ΔNp63 occurs in all surface epithelial cells preparing to undergo desquamation, suggesting a potential role for ΔNp63 isoforms in mediating surface cell apoptotic shedding. In this study, the authors investigated a role for ΔNp63 isoforms in caspase-mediated apoptosis in a telomerase-immortalized corneal epithelial cell line.

Methods. For in vitro studies, hTCEpi cells were cultured in KGM-2 serum-free culture media containing 0.15 mM calcium. To assess dynamic protein interactions among individual ΔNp63 isoforms, ΔNp63-EGFP expression plasmids were transiently expressed in hTCEpi cells and evaluated by FRAP. Trichostatin-A (TSA; 3.31 μM) was used to induce cell death as measured by caspase activity. Cleavage and loss of endogenous ΔNp63α, ΔNp63-EGFP expression plasmids, and p53 were assessed after treatment with TSA and siRNA.

Results. Transient expression of ΔNp63-EGFP α and β isoforms resulted in the formation of a smaller isoform similar in size to ΔNp63γ-EGFP. FRAP demonstrated that ΔNp63α-EGFP has greater immobile fraction than β or γ. TSA induced caspase-mediated apoptotic pathways; caspase induction was accompanied by a decrease in endogenous ΔNp63α and p53. TSA upregulated ΔNp63-EGFP plasmid expression; this was accompanied by a selective increase in cleavage of ΔNp63α-EGFP. siRNA knockdown of ΔNp63α correlated with a reduction in p53 independently of TSA.

Conclusions. ΔNp63α is the dominant active isoform in corneal epithelial cell nuclei. Loss of ΔNp63α occurs during apoptotic signaling by cleavage at the C terminus. The corresponding loss of p53 suggests that a significant relationship appears to exist between these two regulatory proteins. (*Invest Ophthalmol Vis Sci.* 2010;51:3977–3985) DOI:10.1167/iovs.09-4919

A physiologically intact corneal epithelium is essential for optical clarity and for providing a barrier to invasive microorganisms. Survival or homeostatic maintenance of the epithelium is dependent on a small population of lineage-restricted multipotent stem cells harbored in the basal layer of the limbus.[1,2] Cells within this compartment are slow cycling and undergo continuous asymmetric division, giving rise to transient amplifying daughter cells that replenish the epithelium.[3] From the limbus, cells migrate centripetally across the cornea, where they undergo a final round of cell division before ascending vertically toward the corneal surface and ultimately are shed into the precorneal tear film.[4,5] This processes of corneal epithelial cell shedding, or desquamation, has been shown to be regulated by apoptotic mechanisms.[6]

Recent studies[7] in our laboratory have focused on the expression and localization of the transcription factor ΔNp63 in the corneal epithelium. A homologue of the p53 tumor suppressor, ΔNp63, is expressed within tissues that are highly regenerative, such as the basal layer of the skin and in animal models has been shown to be critical to the development of stratified epithelia.[8–10] In the corneal epithelium, ΔNp63 was first thought to reside exclusively in the basal cell layer in the limbus.[11,12] Later reports, however, extended this localization to include the peripheral and central corneal epithelium with a loss of expression in central superficial epithelial cells, cells presumably preparing to desquamate.[7,13–15] In vitro, ΔNp63 is abundantly expressed in nondifferentiated cells and is downregulated on calcium-induced differentiation.[7,16] These findings suggest multiple roles for ΔNp63 in the corneal epithelium as a key regulator of early-onset differentiation from stem cell to transient amplifying cell, a potential role in cell survival, and a role as a mediator for apoptotic-driven surface cell shedding.

Ambiguity in the understanding of the function of ΔNp63 arises from the presence of multiple isoforms of the *p63* gene product. Transcription of *p63* at the promoter upstream of exon 1 encodes for the transactivating or TA isoform which can bind and activate p53 target sites; a second intronic promoter results in the production of the N-terminally deleted or ΔN isoform, initially thought to be transcriptionally inactive, thereby functioning through a dominant negative effect.[17] More recently, a second transactivation domain within the first 26 amino acids of the ΔN isoform has been identified, conferring on ΔNp63 the ability to transactivate p53 target genes, including a lengthening list of apoptotic regulators.[18] At the C terminus, both isoforms are again alternatively spliced, resulting in three additional variants: α, β, and γ. ΔNp63α, which is the predominant isoform in the corneal epithelium, differs from β and γ in the presence of a sterile alpha motif within exon 14 and a C-terminal inhibitory domain, contributing to the complex regulatory functions of this protein.[7,19–22]

Because of the high levels of ΔNp63 seen in many epithelial cancers, the mechanism by which ΔNp63 may mediate cell survival has become an area of heightened interest.[23] Results from these studies have generated conflicting arguments for the function of TA and ΔNp63 isoforms in apoptosis and the ability to regulate downstream apoptotic target genes. In bladder and lung cancer cell lines, expression of ΔNp63 has been shown to confer resistance to apoptosis, whereas loss of ex-

From the Department of Ophthalmology, The University of Texas Southwestern Medical Center, Dallas, Texas.

Supported in part by National Institutes of Health Grant R01 EY018219 (DMR) and Infrastructure Grant EY016664; American Optometric Foundation (DMR); OneSight Research Foundation (DMR); a Research to Prevent Blindness Career Development Award (DMR); and an unrestricted grant from Research to Prevent Blindness.

Submitted for publication November 13, 2009; revised February 21, 2010; accepted March 6, 2010.

Disclosure: **D.M. Robertson**, None; **S.-I. Ho**, None; **H.D. Cavanagh**, None

Corresponding author: Danielle M. Robertson, Department of Ophthalmology, UT Southwestern Medical Center, 5323 Harry Hines Boulevard, Dallas, TX 75390-9057; danielle.robertson@utsouthwestern.edu.

TABLE 1. Primer Sequences for ΔNp63 Isoforms

Primer	Sequence	Temperature (°C)
ΔN Forward	5′-GAA GAT CTA GCC AGA AGA AAG GAC AGC AGC AT-3′	64
α Reverse	5′-AAT CTG CAG TCA CTC CCC CTC CTC TTT GAT GC-3′	67.5
β Reverse	5′-AAC TGC AGT CAG ACT TGC CAG ATC CTG ACA ATC-3′	68
γ Reverse	5′-ATA CTG CAG CTA TGG GTA CAC TGA TCG GTT TGG-3′	68.5

Primers used for generating ΔNp63 isoforms α, β, and γ were determined using published sequences in the NCBI database: GenBank accession numbers AF075431 (α), AF075433 (β), and AF075429 (γ). Primers were synthesized by Integrated DNA Technologies (Coralville, IA). The same forward primer was used for all three isoforms.

pression is necessary for the activation of cell death pathways.[24] Similarly, in the mouse epidermis, the downregulation of ΔNp63 before apoptosis has been demonstrated after UV-B exposure.[25] In contrast, studies examining ΔNp63 expression in primary cultured human foreskin keratinocytes, immortalized human keratinocytes, and a facial squamous cell carcinoma cell line have shown that overexpression of ΔNp63 induces caspase-mediated apoptotic signaling events.[26] These latter findings are further supported by investigations demonstrating that both TA and ΔN variants induce apoptosis in non–small cell carcinoma cells.[18] Significantly, the collective results from all these studies support the view that ΔNp63 activates or inhibits apoptosis in a cell- and tissue-type specific manner.

In the human corneal epithelium, a role for ΔNp63 in regulating cell survival has not yet been investigated. Further, the specific function of the C terminus isoforms of ΔNp63 is unknown. In the present study, we investigated a role for ΔNp63 isoforms in caspase-mediated apoptosis in a telomerase-immortalized human corneal epithelial cell line previously characterized in detail.[27]

MATERIALS AND METHODS

Cell Culture

Human telomerase-immortalized corneal epithelial cells (hTCEpi) were initially isolated and thereafter routinely maintained in KGM-2 serum-free culture media (Clonetics-BioWhittaker, San Diego, CA) containing 0.15 mM calcium, as previously described.[27] Cells were subcultured on tissue culture flasks (T75; Falcon Labware, BD Biosciences, Bedford, MA), incubated at 37°C in 5% CO_2 and passaged every 7 to 10 days. Human telomerized corneal fibroblasts (HTK, generously provided by Matthew Petroll) were used as a control cell line in siRNA experiments. HTK culture conditions are described in detail elsewhere.[28]

EGFP Plasmid Construction

ΔNp63 plasmids were constructed and sequence verified according to GenBank accession numbers AF075431 (α), AF075433 (β), and AF075429 (γ). RNA and cDNA were prepared as previously described.[7] Gene-specific primers for each isoform, including restriction enzyme sites, are listed in Table 1. A 50-μL PCR reaction was performed as follows: 0.5 μM each primer, 0.20 mM dNTPs, 5 μL of 10× PCR buffer (Sigma, St. Louis, MO), 7.5 mM $MgCl_2$ (Sigma), 1 μL DNA polymerase (*Taq*, 5 U/μL; Sigma), and 2 μL cDNA. Reaction conditions for PCR were initial denaturation for one cycle at 94°C for 3 minutes, followed by 25 cycles at 94°C for 1 minute, 60°C for 45 seconds, 72°C for 45 seconds, and a final extension at 72°C for 7 minutes. PCR products were visualized on an ethidium-bromide–stained 1.25% agarose gel under UV light and were PCR purified (QIAQuick PCR purification kit; Qiagen Sciences, Valencia, CA). PCR inserts and the pEGFP-C1 (Clontech, Mountain View, CA) vector were digested using Bgl*II* and Pst*I* restriction enzymes (New England Biolabs, Ipswich, MA). For insert digestion, a 30-μL reaction mixture containing 10 μL DNA, 3 μL of 10× buffer (New England Biolabs), and 1 μL each restriction enzyme was incubated for 2 hours at 37°C. For vector digestion, a 100-μL reaction mixture containing 10 μL plasmid, 10 μL of 10× buffer, and 3 μL each restriction enzyme was incubated for 2 hours at 37°C. After digestion, resultant products were resolved on a 1.25% ethidium bromide–stained agarose gel and purified (QIAquick Gel Extraction Kit; Qiagen Sciences). The cDNA for each insert was ligated into the cut pEGFP-C1 expression plasmid in a 15-μL reaction containing a 1:3 ratio of vector/insert, 1 μL T4 DNA ligase, and 1.5 μL T4 DNA ligase buffer (Invitrogen, Carlsbad, CA) overnight at room temperature. Plasmids were transformed using NEB 5-α competent *Escherichia coli* according to manufacturer's instructions (New England Biolabs). Seventy-five microliters of the resultant mixture was spread onto LB agar plates containing 20 μg/mL kanamycin and incubated overnight at 37°C. Selected clones were grown overnight in 50-mL conical tubes at 37°C with agitation. Clones were purified from *E. coli* (QIAprep Spin Miniprep Kit; Qiagen Sciences), screened by enzyme digestion, and visualized by ethidium bromide–stained 1.25% agarose gel. All plasmids were sequencing confirmed at the McDermott Center for Human Growth and Development, UT Southwestern Medical Center (Dallas, TX). For transient transfection assays, 5 μL overnight broth was grown in 500 mL LB broth containing kanamycin and purified with a plasmid kit (High Pure Plasmid Isolation Kit [Roche Diagnostics, Indianapolis, IN] or QIAfilter Plasmid Maxi Kit [Qiagen Sciences]). DNA concentration was measured by absorbance at 260 nm with a spectrophotometer (DU 530; Beckman Coulter, Hialeah, FL) and was converted to micrograms per microliter.

Overexpression Studies

For overexpression studies, 2.4×10^5 cells/well were plated into six-well plastic tissue culture dishes containing 1 mL antibiotic-free medium. On day 2, hTCEpi cells at 60% to 70% confluence were transfected with one of the following plasmids: pEGFP-ΔNp63α, pEGFP-ΔNp63β, pEGFP-ΔNp63γ, or pEGFP. Four microliters of transfection agent (FuGeneHD; Roche) was added to 50 μL antibiotic-free culture medium in disposable glass culture tubes (Kimble Glass Inc., Vineland, NJ). In separate tubes, 1.25 μg plasmid was added to 50 μL antibiotic-free medium and allowed to incubate at room temperature for 5 minutes. Tubes containing transfection agent (FuGeneHD; Roche) and plasmid were mixed together and allowed to incubate for 25 minutes at room temperature. The resultant mixture was added to the cell culture well and evenly mixed. Transfected cells were imaged on an inverted epifluorescent microscope (Eclipse TE300; Nikon, Melville, NY), and images were acquired with a camera (CoolSnap HQ; Photometrics, Tucson, AZ). Relative transfection efficiencies were obtained by visual approximation. Protein expression was assessed at 24 or 48 hours after transfection and subjected to Western blot analysis.

Fluorescence Recovery after Photobleaching

Fluorescence recovery after photobleaching (FRAP) was used to measure protein dynamics of ΔNp63 isoforms within the nuclear compartment. For FRAP experiments, 2.2×10^5 cells were plated onto glass tissue culture dishes (ΔT4; Bioptics, Tucson, AZ) and were allowed to adhere for 24 hours. hTCEpi cells were transfected with pEGFP-ΔNp63α, pEGFP-ΔNp63β, pEGFP-ΔNp63γ, or pEGFP using transfection reagent (FuGene6; Roche). FRAP studies were performed 24 hours after transfection on a laser scanning confocal microscope (SP2; Leica

Microsystems, Heidelberg, Germany). All images were acquired bidirectionally in fly mode (Confocal Software FRAP Wizard; Leica); 256 × 512 images were acquired at 1000 Hz, excitation 488 nm, at 4% laser power, zoom 8, line average 2. For photobleaching, three excitation wavelengths (458 nm, 476 nm, and 488 nm) were set to 100% to bleach a 2-μm diameter circular region of interest. Before bleaching occurred, five prebleach scans were acquired to establish baseline fluorescence intensity, followed by 2.46 seconds of bleaching. Recovery was monitored until a recovery plateau was achieved. Raw intensity values were exported into spreadsheet software (Excel; Microsoft, Redmond, WA), background subtracted, and corrected for photobleaching effects during scanning. Ten cells per plasmid were examined. Three separate FRAP experiments were performed.

siRNA Knockdown

Predesigned siRNA targeting ΔNp63 was used to knock down all three ΔNp63 isoforms (Silencer; AM16708A; Applied Biosystems, Carlsbad, CA). For all experiments, hTCEpi cells were seeded onto plastic six-well tissue culture dishes (2.2×10^5 cells per well) in antibiotic-free media. Cells were allowed to attach overnight at 37°C in 5% CO_2. siRNA oligonucleotide optimal concentration was empirically determined. In separate tubes, 1 μL of 40 μM siRNA was diluted in 50 μL medium (Opti-MEM; Invitrogen), and 4 μL transfection reagent was diluted in 50 μL medium (Opti-MEM; Invitrogen) and allowed to sit for 5 minutes. Contents were then combined and incubated at room temperature for 25 minutes. The resultant 200 μL siRNA/transfection reagent solution was added directly to the well with antibiotic-free media for a total volume of 1 mL; siRNA oligonucleotides were transfected (Oligofectamine; Invitrogen). Cells were collected at 24 hours after transfection. Efficacy of knockdown was evaluated by Western blot analysis. To control for off-targeting effects, HTK cells that did not express ΔNp63 were transfected under identical conditions to the hTCEpi cell line and assessed for p53 expression.

Protein Extraction and Western Blot Analysis

Total protein was collected by lysing cells in radioimmunoprecipitation buffer containing a protease inhibitor cocktail tablet (Complete-Mini; Roche Diagnostics) on ice for 10 minutes. Lysates were snap frozen in liquid nitrogen, vortexed, and briefly centrifuged to remove the precipitate. All lysates were boiled for 5 minutes in 4× sample buffer (pH 6.8) containing 0.25 M Tris, 8% lauryl sulfate, 40% glycerol, 20% mercaptoethanol, and 0.04% bromophenol blue, resolved on a 7.5% to 10% SDS gel and subsequently transferred to a nitrocellulose membrane. Membranes were blocked in 5% nonfat milk for 1 hour at room temperature and were blotted using the following mouse monoclonal antibodies: antibody clone 4A4 directed against pan-ΔNp63 isoforms (Santa Cruz Biotechnology, Santa Cruz, CA), p53 (Calbiochem, San Diego, CA), actin (Sigma-Aldrich), and EGFP (Covance Research Products, Denver, PA) overnight at 4°C. After 1-hour incubation with an anti–mouse secondary antibody (1:5000 dilution; Amersham Biosciences, Piscataway, NJ), protein was visualized using detection reagents (ECL Plus; Amersham Biosciences) and imaged (Typhoon Variable Mode Imager; GE Healthcare Life Sciences, Little Chalfont, UK).

Caspase-3 Assay

A detection kit (Image-It Live Cell Caspase Assay; Invitrogen) was used to assess caspase-3 activation in hTCEpi cells. Thirty microliters of a 2.4×10^5 cell/mL suspension of hTCEpi cells was seeded onto glass coverslips and allowed to adhere for 24 hours. Cells were treated with 3.31 μM TSA (Sigma) overnight in serum-free KGM2 media. Cells were labeled for caspase-3 according to manufacturer's instructions. Nuclei were counterstained with a 1:1000 dilution of cell-permeable anthraquinone (DRAQ5; Axxora, San Diego, CA) and imaged directly under the laser scanning confocal microscope.

Statistical Analysis

Statistical analysis was performed using commercial software (SigmaStat 3.1; Systat Software, Inc., San Jose, CA). All data are expressed as mean ± SE. Normality and equal variance assumption testing was performed using the Kolmogorov-Smirnov test and the Levene median test. A *t*-test or one- or two-way analysis of variance with an appropriate post hoc multiple comparison test was used to determine which groups were significantly different. Statistical significance was set at $P < 0.05$.

Results

Transient Expression of ΔNp63-EGFP Isoforms

For all transient expression experiments, hTCEpi cells were seeded on plastic and transfected with isoform-specific ΔNp63-EGFP expression plasmids. Relative transfection efficiencies ranged from approximately 60% to 80% for all plasmids tested. A representative region confirming relatively high transfection efficiencies for EGFP in hTCEpi cells grown on a plastic six-well tissue culture dish is shown in Figure 1A. Western blot analysis using a mouse monoclonal antibody directed against the N-terminus of p63 was used to confirm the expression of individual ΔNp63-EGFP isoforms (Fig. 1B). Consistent with our previous reports, ΔNp63α was the predominant endogenous isoform in hTCEpi cells. In cells transfected with ΔNp63-EGFP α, β, or γ, expression of the chimeric protein was seen at 24 and 48 hours. Interestingly, overexpression of ΔNp63α-EGFP and ΔNp63β-EGFP resulted in the formation of a lower molecular weight isoform that appeared to coincide with the size of ΔNp63γ-EGFP (Fig. 1B).

Fluorescence Recovery after Photobleaching

FRAP was performed to establish whether dynamic differences existed in the ability of specific ΔNp63 isoforms to interact with nuclear structures. As expected for a transcription factor, all three isoforms localized exclusively to the nucleus (data not shown). In contrast, the EGFP empty vector control localized diffusely throughout the nucleus and the cytoplasm. For FRAP analysis, a 2-μm diameter circular region of interest in the nuclear compartment was bleached. As shown in Figure 2A, bleaching of ΔNp63α-EGFP produced a 2-μm circular area devoid of EGFP, which appeared to only partially recover over time. ΔNp63β-EGFP and ΔNp63γ-EGFP showed a similar pattern (not shown). In comparison, the EGFP empty vector recovered fluorescence almost instantaneously (Fig. 2A). Analysis of FRAP recovery curves for each isoform compared with the EGFP control demonstrated differences in the amount of recovery among ΔNp63α, β, and γ isoforms (Figs. 2B–D). Notably, ΔNp63α-EGFP appeared to have the least amount of fluorescence recovery, followed by ΔNp63β-EGFP. ΔNp63γ-EGFP showed the greatest recovery of all three proteins but failed to recover completely compared with the freely diffusible EGFP control. It is important to note that estimation of the speed of recovery for ΔNp63α and β isoforms may be confounded in part by the presence of the smaller molecular weight isoform produced after ectopic expression of the EGFP chimeric proteins identified by Western blot analysis in Figure 1B.

Quantitative analysis was used to determine the amount and speed of fluorescence recovery. The amount of fluorescence recovery represents the mobile fraction of the protein, though the difference between the final fluorescence and the initial fluorescence indicates the immobile fraction. As predicted from the FRAP recovery curves in Figure 2, ΔNp63α-EGFP had a significantly greater fraction of immobile protein compared with the other two isoforms and the EGFP control (Fig. 3A; $P < 0.001$, one-way ANOVA), indicating an increase in the amount of physical interactions, either protein-protein or protein-DNA within the nuclear compartment. ΔNp63β-EGFP also had a significantly greater immobile fraction compared with the EGFP control but failed to demonstrate any detectable differ-

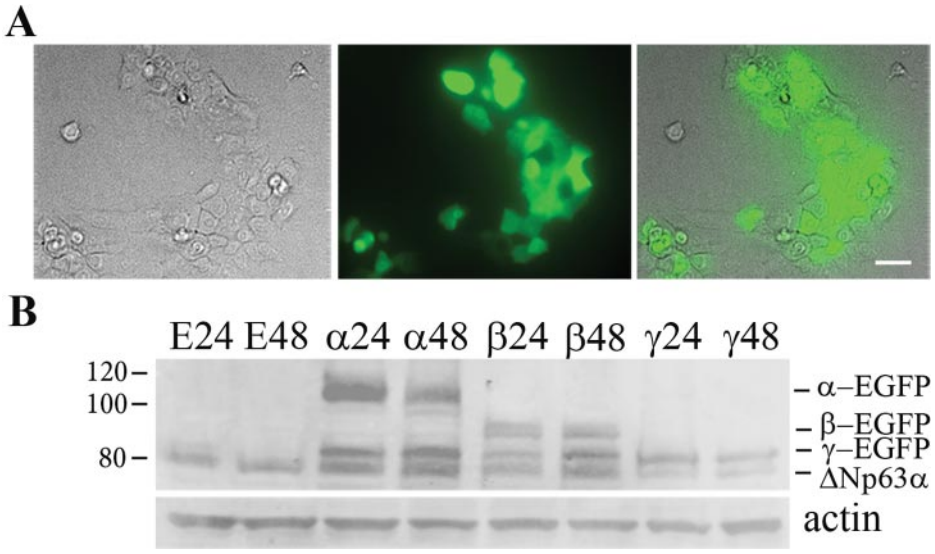

FIGURE 1. Transient overexpression of ΔNp63 isoforms. (**A**) Representative image of transfection efficiency of hTCEpi cells after transient expression with the EGFP empty vector. Nomarski image of hTCEpi cells (*left*), EGFP expression (*middle*), and overlay (*right*). Scale bar, 11.58 μm. (**B**) Western blot for ΔNp63 using the 4A4 monoclonal antibody. Transfection with EGFP expression plasmids encoding the cDNA for ΔNp63 isoforms (*lanes*: E, EGFP empty vector; α, ΔNp63α-EGFP; β, ΔNp63β-EGFP; γ, ΔNp63γ-EGFP; 24, 24 hours after transfection; 48, 48 hours after transfection. *Right of blot*: α-EGFP, β-EGFP, and γ-EGFP represent transfected ΔNp63 plasmids; ΔNp63α denotes the endogenous protein. *Left of blot*: molecular weight markers. Note the enhanced expression of ΔNp63α and ΔNp63β each produced an increase in a protein the same size as ΔNp63γ. Actin was used as a loading control; $n = 3$.

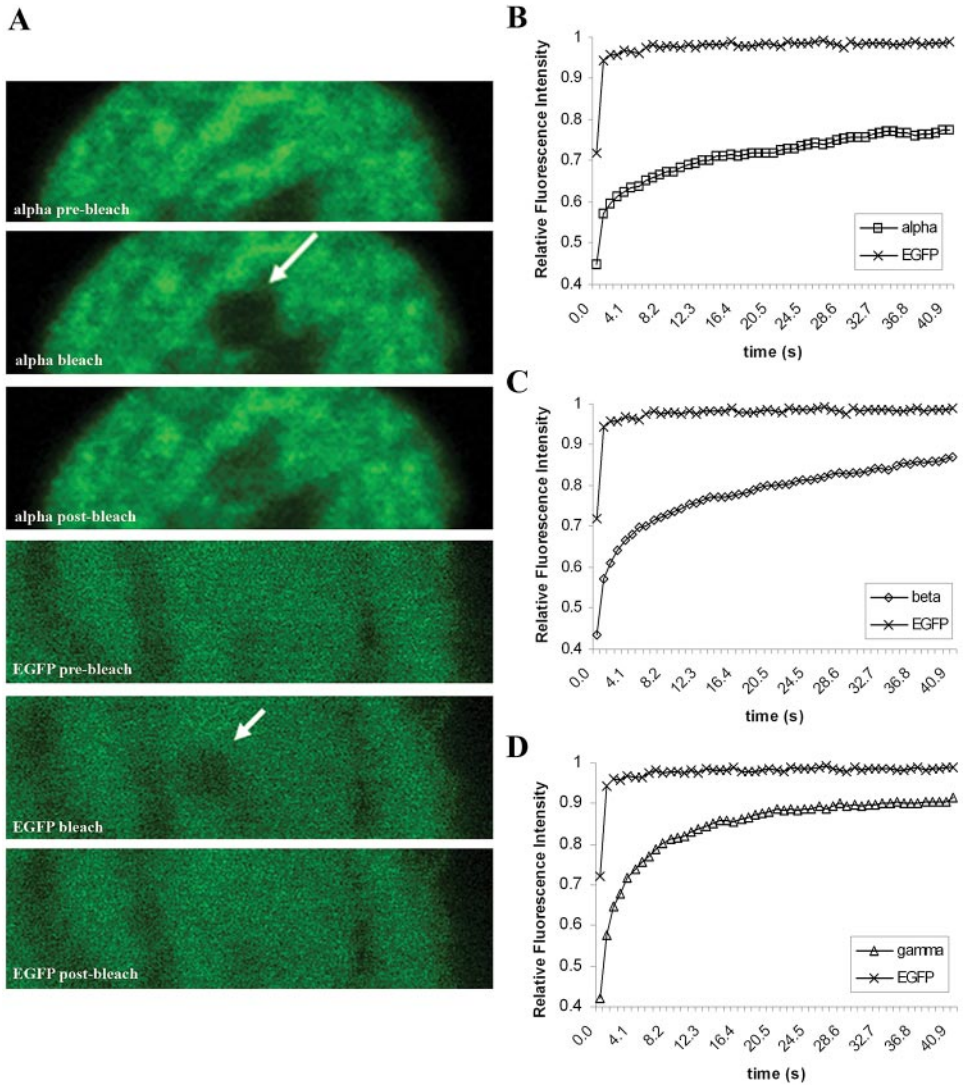

FIGURE 2. FRAP analysis of hTCEpi cells transiently expressing ΔNp63-EGFP expression plasmids. FRAP was used to measure protein mobility within the nuclear compartment. The cell was initially scanned at 4% laser power (4.097 seconds), followed by bleaching a 2-μm diameter circular region of interest (6.555 seconds). Fluorescence recovery was followed over time. *Arrow*: bleached region. (**A**) Top three images representative of an hTCEpi cell expressing ΔNp63α-EGFP before the bleach (pre-bleach), immediately after the bleach (bleach), and at the end of the experimental time course (post-bleach). Note the incomplete recovery in the bleached region. Bottom three images representative of an hTCEpi cell expressing EGFP. (**B–D**) FRAP curves are represented as the mean relative fluorescence intensity as a function of time after bleach. (**B**) ΔNp63α-EGFP compared with EGFP empty vector. (**C**) ΔNp63β-EGFP compared with EGFP empty vector. (**D**) ΔNp63γ-EGFP compared with EGFP empty vector. Ten cells per expression plasmid were analyzed in each experiment; the entire experiment was repeated three times.

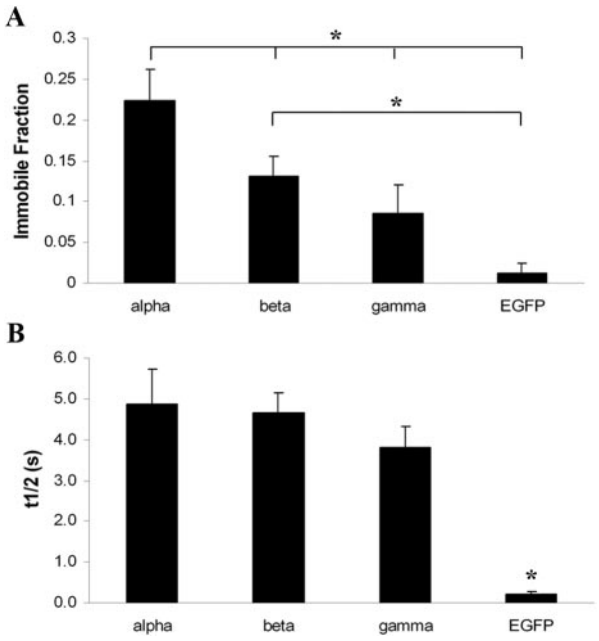

FIGURE 3. Quantitative FRAP analysis of ΔNp63 isoforms in corneal epithelial cell nuclei. All measurements were background subtracted and corrected for photobleaching effects during scanning. (**A**) Calculation of the immobile fraction showed a significantly greater immobile fraction for ΔNp63α than for ΔNp63β, ΔNp63γ, or the EGFP empty vector. ΔNp63β also showed a greater immobile fraction than the EGFP empty vector ($n = 10$; $^*P < 0.001$, one-way ANOVA; SNK multiple comparison test results shown on graph). (**B**) The recovery half-life showed a significantly decreased speed of recovery for all three isoforms examined compared with the EGFP empty vector ($n = 10$; $^*P < 0.001$, one-way ANOVA; SNK multiple comparison test results shown on graph). There was no detectable difference in speed between isoforms.

ence from ΔNp63γ-EGFP. In terms of speed of recovery, the half-time of fluorescence recovery was calculated for each protein by fitting single exponentials to individual recovery curves. The half-time was then calculated based on the time it took for the fluorescence intensity to reach half the recovered intensity. For all three isoforms, the speed of the protein was significantly reduced compared with the EGFP control (Fig. 3B; $P < 0.001$, one-way ANOVA). There was no significant difference in half-time of recovery between individual isoforms.

Caspase Activation

We have previously reported that TSA induces apoptosis in hTCEpi cells using annexin V and TUNEL.[7] To assess whether TSA-induced cell death occurs by way of a caspase-mediated apoptotic pathway, caspase activity was evaluated in hTCEpi cells after overnight incubation in 3.31 μM TSA. Using a live fluorescence cell marker for caspase-3 activity (Fig. 4A), in the nontreated control only an occasional cell demonstrated positive caspase activation. In stark contrast, incubation in TSA resulted in robust caspase activity with most cells positive for caspase (Fig. 4B). Quantitation of the percentage of caspase-positive cells confirmed a significant activation of caspase-3 in TSA-treated cells compared with untreated cells (Fig. 4C; $P < 0.001$, *t*-test).

Trichostatin-A

To assess whether TSA-induced caspase activation was associated with changes in endogenous ΔNp63α expression, hTCEpi cells were treated with 3.31 μM TSA overnight and assessed by Western blot analysis. Compared with nontreated cells, incubation in TSA resulted in a significant decrease in ΔNp63α ($P = 0.029$, *t*-test; Figs. 5A, 5B). Given that interactions between p63 and the p63 homologue p53 have been suggested in other cell lines,[29,30] we further evaluated the effect of TSA on p53. Notably, Western blot analysis for p53 demonstrated a significant decrease in p53 in TSA-treated cells that corresponded with the TSA-stimulated decrease in endogenous ΔNp63α (Figs. 5A, 5C; $P = 0.002$, *t*-test,).

To examine a potential mechanism for the loss of endogenous ΔNp63α, we further explored the effect of TSA on transiently expressed ΔNp63-EGFP chimeric proteins. As shown in Figure 6A, cotreatment of 3.31 μM TSA with transient expression of ΔNp63-EGFP isoforms resulted in several notable effects. First, TSA treatment appeared to upregulate ΔNp63-EGFP plasmid expression for all three expression plasmids tested. Analysis of each expression plasmid treated with TSA compared with the same plasmid expressed in the absence of TSA demonstrated a significant increase in protein expression (Figs. 6B–D; $P = 0.029$ [α, β, γ], *t*-test,). The second finding demonstrated an increase in the smaller molecular weight isoform previously reported in Figure 1B after transient expression of ΔNp63α-EGFP that was consistent with the size of ΔNp63γ-EGFP. Expression of this smaller isoform was significantly greater than that seen in the non–TSA-treated group (Fig. 6E; $P = 0.029$, *t*-test). A similar increase in cleavage of ΔNp63β-EGFP was also noted (Fig. 6F; $P = 0.029$, *t*-test). Analysis of the ratio of cleaved protein to expressed protein for α and β isoforms showed a significant increase in cleavage of ΔNp63α after treatment with TSA (Fig. 6G; $P = 0.029$, *t*-test). There was no significant difference in the ratio of cleaved to expressed ΔNp63β with or without TSA treatment (Fig. 6H; $P = 0.343$, *t*-test).

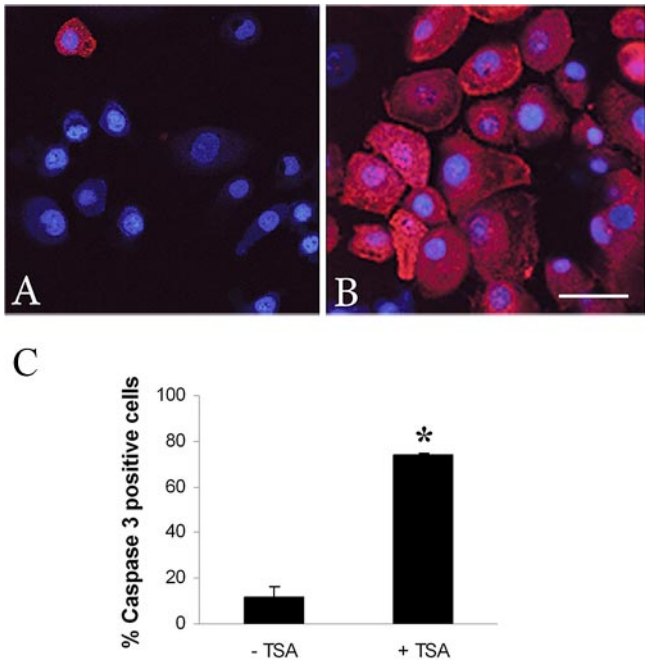

FIGURE 4. TSA-induced caspase activity. (**A**, **B**) hTCEpi cells labeled with detection kit (*red*) and DRAQ5 (cell-permeable nuclear stain in *blue*) after incubation in TSA. Scale bar, 35 μm. (**A**) No TSA. (**B**) 3.31 μM TSA. (**C**) A significant increase in caspase-3 activity was seen after treatment with TSA ($n = 3$. Significance compared with non-TSA–treated group; $^*P < 0.001$, *t*-test).

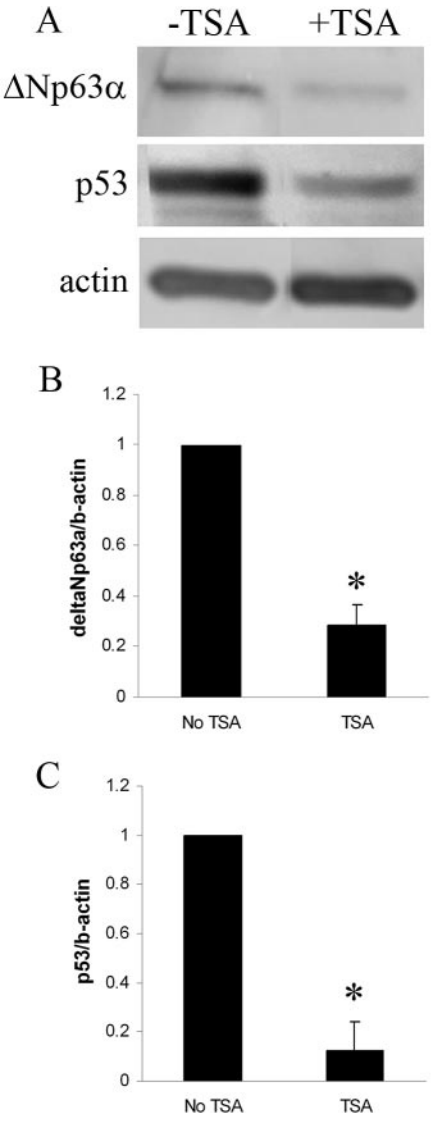

FIGURE 5. TSA-mediated changes in hTCEpi cells. (**A**, *top*) Western blot for ΔNp63α without (−TSA) and with (+TSA) incubation in 3.31 μM TSA demonstrated a decrease in endogenous expression of ΔNp63α. *Middle*: Western blot for p53 demonstrated a corresponding decrease in p53 after TSA treatment. *Bottom*: actin was used as a loading control in all experiments. Experiments were performed three or four times. (**B**, **C**) Quantitative analysis of changes in protein expression. (**B**) Endogenous ΔNp63α was significantly decreased after incubation in TSA ($n = 4$; $^*P = 0.029$, *t*-test). (**C**) Similar to ΔNp63α, a significant reduction in p53 was seen after treatment with TSA ($n = 3$; $^*P = 0.002$, *t*-test).

Cleavage of ΔNp63

The identity of the lower molecular weight isoform produced after ΔNp63α-EGFP and ΔNp63β-EGFP overexpression was further evaluated by Western blot analysis using a mouse monoclonal antibody directed against EGFP (Fig. 7A). As expected, expression of the EGFP empty vector resulted in a small molecular weight band of approximately 27 kDa. The EGFP antibody also confirmed the expression of the three ΔNp63-EGFP chimeric proteins and the two smaller cleavage bands formed from ΔNp63α-EGFP and ΔNp63β-EGFP. Examination of the linear vector maps for each of the fusion proteins demonstrated that EGFP was attached to the N-terminal side of each isoform (Fig. 7B). Based on the protein map, ΔNp63α-EGFP and ΔNp63β-EGFP recombinant proteins were cleaved within the C terminus (Fig. 7C).

siRNA

To examine the relationship between endogenous ΔNp63α and p53 in the absence of compounding effects from TSA, siRNA targeting the noncoding region at the C terminus of ΔNp63 was used. As shown in Figure 8, siRNA produced efficient knockdown of ΔNp63α, which resulted in a corresponding decrease in p53 (Figs. 8A, 8B; $P < 0.001$, two-way ANOVA). Further analysis of the reduction in ΔNp63α with p53 demonstrated a significant correlation between the expression of the two proteins (Fig. 8C; $R^2 = 0.906$; $P = 0.034$, Pearson product moment correlation). To control for off-targeting effects, HTK cells that do not express ΔNp63α were simultaneously transfected with ΔNp63 siRNA oligonucleotides. At 24 hours after transfection, p53 levels were unchanged (Fig. 9).

DISCUSSION

In the human corneal epithelium, ΔNp63, a closely related p53 family member, has been previously highlighted as a key limbal stem cell marker with a widely accepted role in regulating the proliferative capacity of limbal epithelial stem cells in tissue and cell culture studies alike.[11,12] Since those early studies, additional reports have introduced conflicting evidence for an exclusive role for ΔNp63 within the limbal stem cell niche through the demonstration of ΔNp63 transcripts outside the limbal stem cell compartment.[13] In line with these findings, results from our in situ proteomic studies have further confirmed that ΔNp63 isoforms are retained and expressed throughout the central corneal epithelium.[7] Significantly, the loss of expression of ΔNp63 was restricted solely to superficial cells, cells presumably preparing to desquamate, creating new possibilities for the potential function(s) for ΔNp63 in mediating epithelial differentiation and survival outside the limbal stem cell niche.

ΔNp63α Nuclear Dynamics

ΔNp63 is a transcription factor that resides exclusively in the nuclei of all corneal epithelial cells in vitro, regardless of mitotic state.[7] Transient transfection of ΔNp63-EGFP isoforms confirms this localization pattern for all three established splice variants; however, the functional significance of the individual proteins in the corneal epithelium has not been established. In this study, we investigated the nuclear dynamics of ΔNp63 isoforms in hTCEpi cells using FRAP, a kinetic microscopy technique established as a measure of protein mobility within subcellular compartments, which can be used to provide insight into specific protein interactions.[31,32] Within the nucleus, nuclear proteins such as transcription factors typically exhibit a high degree of mobility.[33] This high level of protein mobility likely reflects transient nuclear interactions as opposed to slower moving and immobile proteins, which are presumably undergoing oligomerization or more stable binding to intracellular structures. In contrast, compared with the freely diffusible EGFP, transcription factors that appear highly mobile will exhibit some degree of reduced mobility. In this study, FRAP curves for individual ΔNp63 isoforms all demonstrated a relatively quick fluorescence recovery characteristic of transcription factor binding behavior; however, overall protein mobility was reduced compared with EGFP. Further, differences in the average FRAP recovery curves for specific isoforms indicated that ΔNp63α undergoes a significantly greater degree of nuclear binding interactions than the other two isoforms. Previous studies have demonstrated that substantial changes in nuclear binding activity are evident by small alterations in the FRAP curve.[33] Thus, the significant differences seen in our FRAP findings support the view that ΔNp63α is the predominant interacting isoform in the corneal epithelial nucleus.

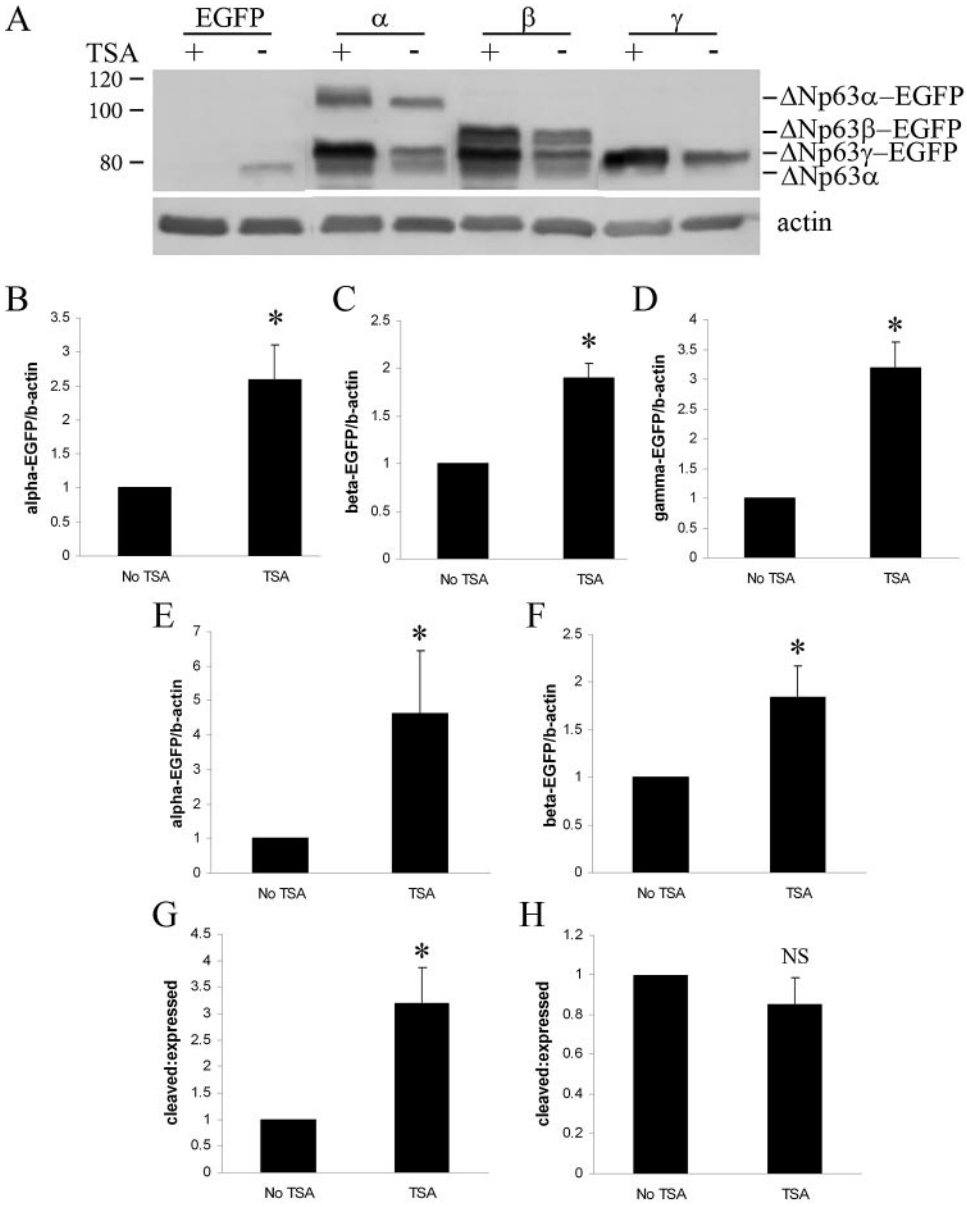

FIGURE 6. The effect of TSA on ΔNp63-EGFP plasmid expression. (**A**) Western blot for ΔNp63 after transfection of ΔNp63 isoforms. Cells were incubated in 3.31 μM TSA. +, with TSA; −, without TSA; EGFP, empty vector; α, ΔNp63α-EGFP; β, ΔNp63β-EGFP; γ, ΔNp63γ-EGFP. *Right*: ΔNp63α denotes endogenous protein expression. Expression of chimeric-EGFP expression plasmids shown. *Left*: molecular weight markers. Actin was used as a loading control for the identical samples above. All experiments were performed four times. (**B–H**) Quantitative analysis of changes in protein expression after incubation in TSA. (**B–D**) ΔNp63-EGFP expression plasmids showed higher levels of expression after treatment with TSA. Given that cells were transfected before the addition of TSA, this effect could not have been caused by an alteration in transfection efficiency from TSA ($n = 4$; $^*P = 0.029$, *t*-test). Because of the potential for variation in transfection efficiency among plasmids, comparisons were limited to individual plasmids with and without treatment. (**E**, **F**) There was a significant increase in the smaller isoform after transfection with ΔNp63α-EGFP and ΔNp63β-EGFP when treated with TSA ($n = 4$; $^*P = 0.029$, *t*-test). (**G**, **H**) Evaluation of the ratio of cleaved protein (smaller isoform) to expressed protein demonstrated that TSA selectively increased the cleavage of ΔNp63α-EGFP compared with ΔNp63β-EGFP. (**G**) $n = 4$, ΔNp63α-EGFP; $^*P = 0.029$. (**H**) ΔNp63β-EGFP; $P = 0.343$, *t*-test.

Loss of Endogenous ΔNp63α

We have previously shown that incubation of hTCEpi cells in TSA induces apoptotic-mediated cell death as measured by annexin V and TUNEL assays.[34] In this study, we demonstrated that treatment with TSA is associated with apoptosis through the activation of caspase. Significantly, treatment with TSA was also associated with a concurrent downregulation of endogenous ΔNp63α. Given the widespread effect of TSA on histone acetylation and genomic methylation, the signaling pathway responsible for inducing caspase-mediated apoptotic cell death may occur independently of the loss of ΔNp63α; however, compared with our previously reported in vivo results confirming the loss of ΔNp63α in the superficial cell layer of the corneal epithelium,[7] these findings suggest that the loss or degradation of ΔNp63α may play a vital role in regulating the susceptibility of the cell to an apoptotic stimulus or that it occurs as part of the apoptotic process.

Of interest in this study, the reported TSA-associated decrease in ΔNp63α also corresponded to a reduction in p53 expression levels. This interaction was confirmed to be a direct effect of the loss of ΔNp63α and not an artifact of TSA treatment because siRNA knockdown of endogenous ΔNp63α significantly correlated with a loss of p53. Although p53 has been previously reported to localize within the corneal epithelium, at present there are no studies characterizing the functional significance of this protein under normal homeostatic conditions.[35] Taken together, these findings indicate that a direct interaction exists between ΔNp63α and p53 in corneal epithelial cells and that this loss occurs during apoptotic-driven cell death. Further studies are necessary to explore the significance of this finding.

Trichostatin A and Ectopically Expressed ΔNp63α

An unexpected result in this study was the upregulation of transiently expressed ΔNp63 isoforms after treatment with TSA. This increased level of ectopic gene expression was likely a result of interactions between TSA and the cytomegalovirus (CMV) immediate early promoter used by our expression plasmid. The ability of TSA to drive the CMV promoter when transfected into mammalian cell lines has been previously reported.[36] Further, it is well established that gene expression is regulated in part by alterations in histone acetylation; however, the exact mechanism by which TSA drives the CMV promoter remains unknown and was beyond the scope of this

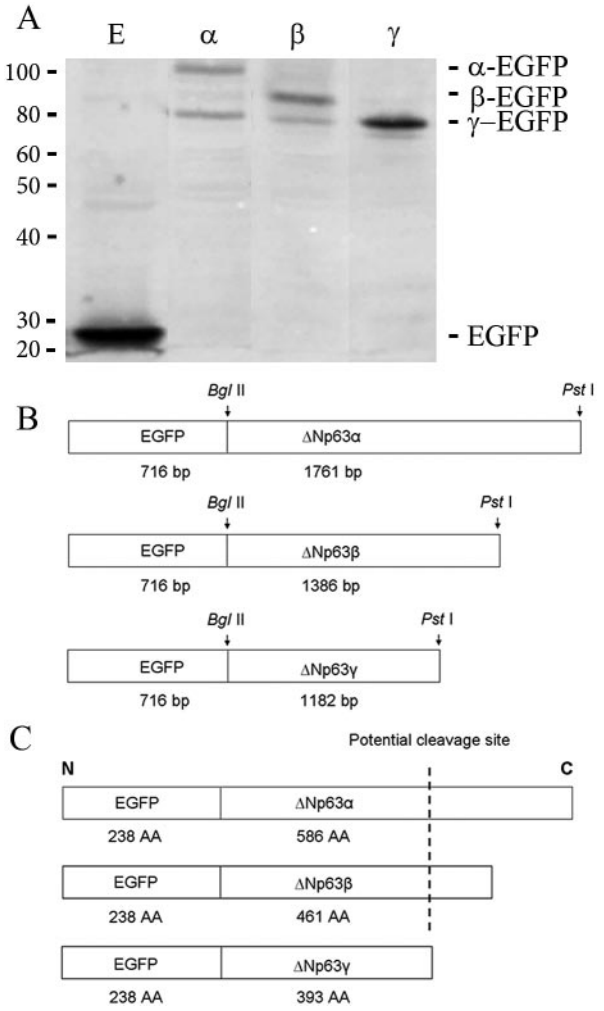

FIGURE 7. Cleavage of ΔNp63-EGFP isoforms. (**A**) Western blot for EGFP confirmed that the lower molecular weight bands present after forced expression of ΔNp63α and ΔNp63β were shortened fragments of the longer ΔNp63-EGFP isoforms (E, EGFP; α, ΔNp63α-EGFP; β, ΔNp63β-EGFP; γ, ΔNp63-EGFPγ). (**B**) Linear vector maps for each ΔNp63-EGFP construct. ΔNp63α, ΔNp63β, and ΔNp63γ cDNA were directionally cloned into the EGFP-C1 expression plasmid using *Bgl*II and *Pst*I restriction sites. (**C**) Protein map for each ΔNp63-EGFP fusion protein. Based on the Western blot in (**A**), a potential cleavage site must exist near the C terminus of both ΔNp63α and ΔNp63β, resulting in an isoform similar in size to ΔNp63γ.

study. Of more significance is the apparent increase in cleavage of ectopically expressed ΔNp63α and ΔNp63β after incubation in TSA. Although cleavage of the α variant of ΔN and TA isoforms has been previously reported, in those studies cleavage was mediated through a caspase cleavage site within the terminal inhibitory domain.[22] Importantly, this domain, though present within the C terminus of ΔNp63α, was not present within the C terminus of ΔNp63β, suggesting the possibility of a second proteolytic cleavage site encoded by both isoforms. Collectively, these results underscore two important findings in this work. First, cleavage was limited to ΔNp63α and ΔNp63β, producing a smaller isoform equivalent to the uncleaved ΔNp63γ, indicating that a proteolytic cleavage site resided within the C terminus of the α and β isoforms that was not present in the γ isoform. Second, specific-TSA–associated cleavage that occurred during caspase-mediated apoptosis appeared restricted to ΔNp63α, and the apparent increase in cleavage of ΔNp63β was an indirect result of the increased levels of plasmid expression.

Overall, our collective in vitro and previous in vivo findings suggest that ΔNp63α is the dominant interacting isoform in corneal epithelial cells and is lost through a yet unidentified proteolytic cleavage mechanism within the C terminus during apoptotic-directed cell death in the corneal epithelium. Further, a novel direct relationship has been identified between ΔNp63α and the classic tumor suppressor p53, opening a new avenue for investigation in elucidating the roles of ΔNp63α in regulating proliferative and apoptotic mechanisms within the corneal epithelium.

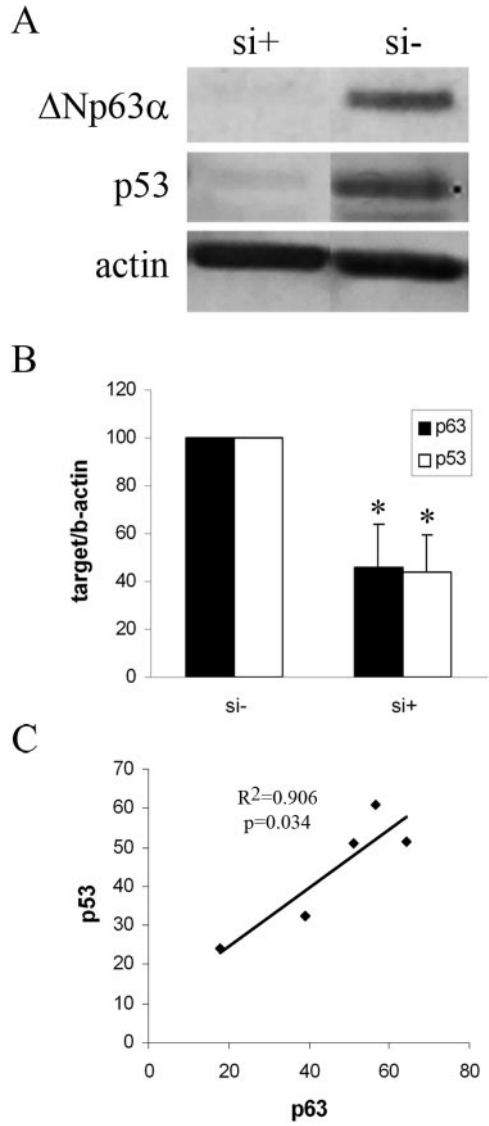

FIGURE 8. siRNA targeting ΔNp63α in the absence of TSA. *Top*: Western blot for ΔNp63α confirming knockdown of protein expression (si+, siRNA; si−, control). *Middle*: Western blot for p53. Loss of endogenous ΔNp63α after siRNA appeared to correspond to a decrease in p53. *Bottom*: actin was used as a loading control. The experiment was repeated five times. (**B**) Quantitative analysis of changes in protein expression showed a significant reduction in endogenous ΔNp63α and p53 after knockdown compared with controls ($n = 5$; $^*P < 0.001$, two-way ANOVA; SNK multiple comparison test). There was no significant difference between ΔNp63α and p53 ($P = 0.863$). (**C**) There was a significant correlation between the expression of p53 and that of ΔNp63α ($n = 5$; $R^2 = 0.906$; $P = 0.034$, Pearson product moment correlation).

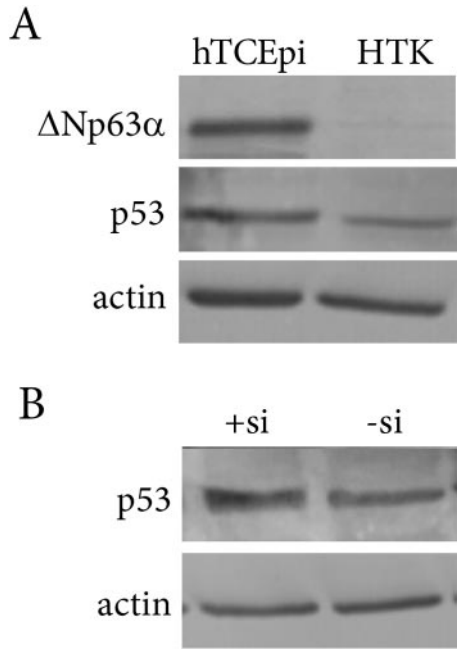

FIGURE 9. siRNA knockdown of ΔNp63 in HTK cells. (**A**) Western blot for ΔNp63 (*top band*) and p53 (*middle band*) in hTCEpi cells and HTK cells. Western blot confirmed the absence of ΔNp63 in HTK cells; p53 expression was seen in both cell lines. (**B**) siRNA knockdown of ΔNp63 in the HTK cell line failed to decrease p53 levels (+si, siRNA; −si, control). Actin was used as a loading control. The experiment was repeated three times.

References

1. Lavker RM, Dong G, Cheng SZ, et al. Relative proliferative rates of limbal and corneal epithelia: implications of corneal epithelial migration, circadian rhythm, and suprabasally located DNA-synthesizing keratinocytes. *Invest Ophthalmol Vis Sci.* 1991;32:1864–1875.
2. Cotsarelis G, Cheng SZ, Dong G, et al. Existence of slow-cycling limbal epithelial basal cells that can be preferentially stimulated to proliferate: implications on epithelial stem cells. *Cell.* 1989;57:201–209.
3. Lavker RM, Tseng SC, Sun TT. Corneal epithelial stem cells at the limbus: looking at some old problems from a new angle. *Exp Eye Res.* 2004;78:433–446.
4. Thoft RA, Friend J. The X, Y, Z hypothesis of corneal epithelial maintenance. *Invest Ophthalmol Vis Sci.* 1983;24:1442–1443.
5. Ladage PM, Jester JV, Petroll WM, et al. Vertical movement of epithelial basal cells toward the corneal surface during use of extended-wear contact lenses. *Invest Ophthalmol Vis Sci.* 2003;44:1056–1063.
6. Ren H, Wilson G. Apoptosis in the corneal epithelium. *Invest Ophthalmol Vis Sci.* 1996;37:1017–1025.
7. Robertson DM, Ho SI, Cavanagh HD. Characterization of DeltaNp63 isoforms in normal cornea and telomerase-immortalized human corneal epithelial cells. *Exp Eye Res.* 2008;86:576–585.
8. Mills AA, Zheng BH, Wang XJ, et al. p63 is a p53 homologue required for limb and epidermal morphogenesis. *Nature.* 1999;398:708–713.
9. Van Bokhoven H, McKeon F. Mutations in the p53 homolog p63: allele-specific developmental syndromes in humans. *Trends Mol Med.* 2002;8:133–139.
10. Yang A, Schweitzer R, Sun DQ, et al. p63 is essential for regenerative proliferation in limb, craniofacial, and epithelial development. *Nature.* 1999;398:714–718.
11. Pellegrini G, Golisano O, Paterna P, et al. Location and clonal analysis of stem cells and their differentiated progeny in the human ocular surface. *J Cell Biol.* 1999;145:769–782.
12. Pellegrini G, Dellambra E, Golisano O, et al. p63 identifies keratinocyte stem cells. *Proc Natl Acad Sci USA.* 2001;98:3156–3161.
13. Kawasaki S, Tanioka H, Yamasaki K, et al. Expression and tissue distribution of p63 isoforms in human ocular surface epithelia. *Exp Eye Res.* 2006;82:293–299.
14. Shanmuganathan VA, Foster T, Kulkarni BB, et al. Morphological characteristics of the limbal epithelial crypt. *Br J Ophthalmol.* 2007;91:514–519.
15. Chang CY, Green CR, McGhee CNJ, et al. Acute wound healing in the human central corneal epithelium appears to be independent of limbal stem cell influence. *Invest Ophthalmol Vis Sci.* 2008;49:5279–5286.
16. King KE, Ponnamperuma RM, Yamashita T, et al. DeltaNp63alpha functions as both a positive and negative transcriptional regulator and blocks in vitro differentiation of murine keratinocytes. *Oncogene.* 2003;22:3635–3644.
17. Yang A, Kaghad M, Wang Y, et al. p63, a p53 homolog at 3q27–29, encodes multiple products with transactivating, death-inducing, and dominant-negative activities. *Mol Cell Biol.* 1998;2:305–316.
18. Dohn M, Zhang S, Chen X. p63alpha and DeltaNp63alpha can induce cell cycle arrest and apoptosis and differentially regulate p53 target genes. *Oncogene.* 2001;20:3191–3205.
19. Thanos CD, Bowie JU. p53 Family members p63 and p73 are SAM domain-containing proteins. *Prot Sci.* 1999;8:1708–1710.
20. Harms KL, Chen X. The C terminus of p53 family proteins is a cell fate determinant. *Mol Cell Biol.* 2005;25:2014–2030.
21. Serber Z, Lai HC, Yang A, et al. A C-terminal inhibitory domain controls the activity of p63 by an intramolecular mechanism. *Mol Cell Biol.* 2002;22:8601–8611.
22. Sayan BS, Sayan AE, Yang AL, et al. Cleavage of the transactivation-inhibitory domain of p63 by caspases enhances apoptosis. *Proc Nat Acad Sci USA.* 2007;104:10871–10876.
23. Westfall MD, Pietenpol JA. p63: molecular complexity in development and cancer. *Carcinogenesis.* 2004;28:857–864.
24. Lee H-O, Lee J-H, Choi E, et al. A dominant negative form of p63 inhibits apoptosis in a p53-independent manner. *Biochem Biophys Res Comm.* 2006;344:166–172.
25. Liefer KM, Koster MI, Wang X-J, et al. Down-regulation of p63 is required for epidermal UV-B-induced apoptosis. *Cancer Res.* 2000;60:4016–4020.
26. Zhu L, Rorke EA, Eckert RL. DeltaNp63alpha promotes apoptosis of human epidermal keratinocytes. *J Invest Dermatol.* 2007;127:1980–1991.
27. Robertson DM, Li L, Fisher S, et al. Characterization of growth and differentiation in a telomerase-immortalized human corneal epithelial cell line. *Invest Ophthalmol Vis Sci.* 2005;46:470–478.
28. Jester JV, Huang J, Fisher S, et al. Myofibroblast differentiation of normal human keratocytes and hTERT, extended-life human corneal fibroblasts. *Invest Ophthalmol Vis Sci.* 2003;44:1850–1858.
29. Djelloul S, Tarunina M, Barnouin K, et al. Differential protein expression, DNA binding and interaction with SV40 large tumour antigen implicate the p63-family of proteins in replicative senescence. *Oncogene.* 2002;21:981–989.
30. Ratovitski EA, Patturajan M, Hibi K, et al. p53 associates with and targets deltaNp63 into a protein degradation pathway. *Proc Natl Acad Sci USA.* 2001;98:1817–1822.
31. Lippincott-Schwartz J, Snapp E, Kenworthy A. Studying protein dynamics in living cells. *Nat Rev Mol Cell Biol.* 2001;2:444–456.
32. Phair RD, Misteli T. High mobility of proteins in the mammalian cell nucleus. *Nature.* 2000;404:604–609.
33. Karpova TS, Chen TY, Sprague BL, et al. Dynamic interactions of a transcription factor with DNA are accelerated by a chromatin remodeller. *EMBO Rep.* 2003;5:1067–1070.
34. Robertson DM, Ho SI, Hansen BS, et al. Insulin-like growth factor binding protein-3 expression in the human corneal epithelium. *Exp Eye Res.* 2007;85:492–501.
35. Tendler Y, Panshin A, Weisinger G, et al. Identification of cytoplasmic p53 protein in corneal epithelium of vertebrates. *Exp Eye Res.* 2006;82:674–681.
36. Spenger A, Ernst W, Condreay JP, et al. Influence of promoter choice and trichostatin A treatment on expression of baculovirus delivered genes in mammalian cells. *Prot Expr Purif.* 2004;38:17–23.